Eur. Phys. J. A **9**, 63–68 (2000)

THE EUROPEAN PHYSICAL JOURNAL A

Two-neutron correlations at small relative momenta in ^{40}Ar + ^{197}Au collisions at 60 MeV/nucleon

J. Pluta[1,a], K. Wosińska[1], Z. Basrak[2], G. Bizard[3], B. Benoit[4], P. Désesquelles[5], O. Dorvaux[6], D. Durand[3], B. Erazmus[7], F. Hanappe[4], B. Jakobsson[8], C. Lebrun[7], F.R. Lecolley[3], R. Lednicky[9], P. Leszczyński[1], K. Mikhailov[10], K. Miller[1], B. Noren[8], T. Pawlak[1], M. Przewłocki[1], Ö. Skeppstedt[11], A. Staranowicz[1], A. Stavinskiy[10], L. Stuttgé[12], and B. Tamain[3]

[1] Warsaw University of Technology, Koszykowa 75, 00-662 Warsaw, Poland
[2] Ruđer Bošković Institute, P.O. Box 180, HR-10 002 Zagreb, Croatia
[3] Laboratoire de Physique Corpusculaire, IN2P3-CNRS, ISMRA et Université, 14 050 Caen cedex, France
[4] Université Libre de Bruxelles, B-1 050 Bruxelles, Belgium
[5] Institut des Sciences Nucléaires, IN2P3-CNRS et Université J. Fourier, 38 026 Grenoble cedex, France
[6] Accelerator Laboratory, University of Jyväskylä, P.O. Box 35, FIN-40 351 Jyväskylä, Finland
[7] Laboratoire SUBATECH, École des Mines de Nantes, IN2P3-CNRS et Université, 44 307 Nantes cedex 03, France
[8] University of Lund, 22 100 Lund, Sweden
[9] Institute of Physics ASCR, Na Slovance 2, 18 221 Prague 8, Czech Republic
[10] Institute for Theoretical and Experimental Physics, Moscow, Russia
[11] Chalmers University of Technology, 412 96 Göteborg, Sweden
[12] Institut de Recherches Subatomiques, IN2P3-CNRS et Université L. Pasteur, 67 037 Strasbourg cedex 2, France

Received: 5 April 2000 / Revised version: 10 July 2000
Communicated by D. Guerreau

Abstract. Two-neutron correlation functions are measured in the ^{40}Ar + ^{197}Au reaction at 60 MeV/nucleon to study the space-time characteristics of neutron emitting sources. The source temperatures and velocities are deduced by fitting the single-neutron energy spectra with a three-source model. A comparison of the correlation data with the predictions of the model of moving sources and with the dynamical Landau-Vlasov model suggests the relevance of a multisource description. Particular care has been paid to the influence of the relative source abundance on the shape of the correlation function.

PACS. 25.70.-z Low and intermediate energy heavy-ion collisions – 25.75.Gz Particle correlations

1 Introduction

Correlations of particles at small relative velocities are widely used to reveal the space-time properties of the emission process in heavy-ion collisions [1]. In the case of charged particles, the long-range Coulomb force from the emitting source and between two charged particles introduces some distortions of the two-particle correlation pattern making the interpretation of the results ambiguous. Two-neutron correlations are free of it. Despite this favourable property, the results on two-neutron correlations are very scarce. The parasite effects in the detection of neutrons in coincidence usually preclude the measurement of two-neutron correlations in the region of small relative momenta. There are some methods of eliminating these parasite effects [2,3]. In this paper the method of [2] is used as it corresponds best to our experimental conditions.

The common tendency, emphasized in many papers on two-nucleon correlations, is the growth of the correlation effect with the increase of emitted particle energy. In the frame of the most straightforward interpretation, this dependence corresponds to the decrease of space-time parameters of particle emission and reflects a relation between the particle momenta and the mechanism of their emission.

However, the attempts to describe the shape of experimentally observed correlation functions with a single curve corresponding to pre-defined space-time parameters appear to be difficult. Frequently, a set of theoretical curves corresponding to a grid of parameter values is superimposed on the experimental result in order to show the scale of effect in relation to different theoretical predictions [4–9]. It seems that the observed correlations originate from averaging over the contributions coming from different sources which cannot be well separated by a simple energy cut. Three distinct sources are conceivable: the pre-equilibrium (PE), the quasi-target (QT) and

[a] e-mail: pluta@if.pw.edu.pl

the quasi-projectile (QP) ones, but with a presumably different contribution to each of particle classes.

In this paper we report the results on the source parameters deduced from an analysis of two-neutron correlation functions. The experimental correlation functions are compared with those obtained using a statistical multisource approach described in sect. 5 and with a dynamical model [10].

2 Experiment

The measurements were performed at the GANIL facility within the E 240 experimental set-up [11]. The reaction studied was ^{40}Ar + ^{197}Au at an incident energy of 60 MeV/nucleon. Emitted neutrons were detected by 97 modules of the DEMON detector [12] installed at about 2 m from the target. The charged-particle component was absorbed, up to 70 MeV, in a lead absorber placed in front of a liquid scintillator container. In addition, the DEMON detectors situated at forward angles were equipped with thin veto plastic scintillators to reject charged particles able to cross the absorber. A block of 12 closely packed modules was used for correlation measurements and served as a neutron interferometer. These modules were mounted at close relative angles and placed at three different distances (150, 200, 250 cm) from the target in order to eliminate the parasite effects following the method of ref. [2]. This neutron interferometer was placed at a mean angle of about 50 degrees with respect to the beam axis. The smallest angle between the detectors was 6° and the neutron kinetic-energy range 5 – 580 MeV.

The trigger conditions, both for inclusive spectra and for correlations, were determined by the registration of heavy fragments using the solid state telescopes installed in the forward direction [11].

The dependence of the experimental two-neutron correlation functions on k^*, the half of momentum difference in the two-neutron rest frame, is presented in fig. 1. Three cuts in neutron energies are indicated. A very strong dependence of the correlation effect on the energy cut is clearly seen. The increase of the correlation effect with increasing neutron energies can be related to the decrease of space-time intervals in the neutron emission process. The origin of neutrons coming from different sources can be deduced from their laboratory energies: low energies correspond predominantly to the target fragmentation, medium-energy neutrons come mostly from the compact system formed at the early stage of the collision, and highest energies can be attributed to the projectile disintegration. The observed tendency is in qualitative agreement with this intuitive expectation. (Note also that we analyze a strongly asymmetric system here.)

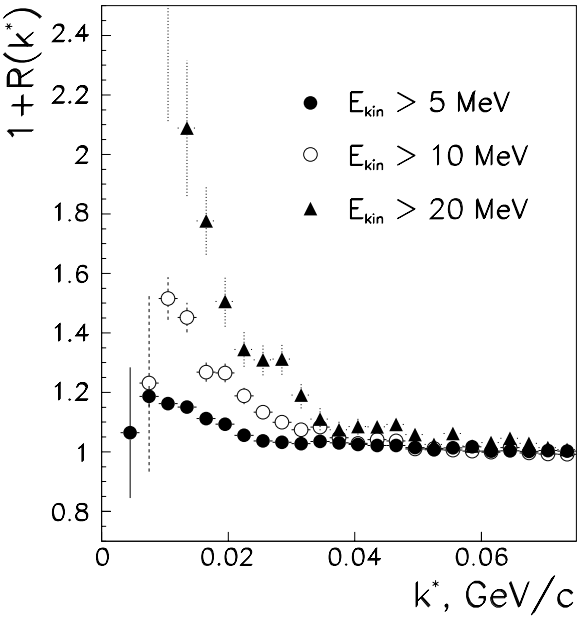

Fig. 1. Dependence of the experimental two-neutron correlation functions on the half of momentum difference, k^*, when both neutrons have a kinetic energy higher than 5, 10 and 20 MeV.

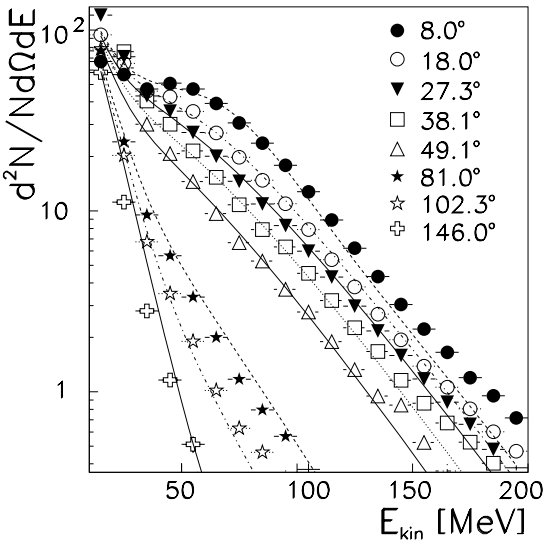

Fig. 2. Neutron energy spectra measured for the emission angles from $\theta = 8°$ to $\theta = 146°$. The curves correspond to the fits with the three-equilibrated-source model, eq. (1).

3 Single-particle inclusive energy spectra

The parameters of the emitting sources were determined using single-particle inclusive energy spectra. It was assumed that registered neutrons were emitted from three equilibrated sources with Maxwellian energy distributions. Temperatures, intensities and velocities in the laboratory system were attributed to each source. A simultaneous fit was performed for a set of angles with the standard formula

$$\frac{\mathrm{d}^2\sigma}{\mathrm{d}E\mathrm{d}\Omega} = \sum_{i=1}^{3} N_i \sqrt{E} \exp\left[-\left(E + E_i - 2\sqrt{E_i E}\cos\Theta\right)/T_i\right], \quad (1)$$

where E and Θ are, respectively, the kinetic energy and the angle of emission of the neutron in the laboratory rest frame, N_i is the normalization constant, T_i the i-th source "temperature" parameter, E_i the part of the neutron kinetic energy related to the source movement ($E_i = mv_i^2/2$, where m is the neutron mass and v_i is the source velocity in the laboratory system). All fitting parameters are free. The best fit of the function (1) to the data is shown in fig. 2. The corresponding parameters are listed in table 1. The errors of the parameters are purely statistical. The agreement is generally good except for neutrons

Table 1. Parameters of the three equilibrated sources, eq. (1), fitted to the inclusive neutron spectra (fig. 2). N_i, v_i and T_i are the normalization constant, velocity (in c units) and temperature (in MeV) of the i-th source, respectively.

Quasi-target		Pre-equilibrium		Quasi-projectile	
N_1	136.2 ± 0.6	N_2	11.19 ±0.02	N_3	2.27 ±0.02
v_1	0.0 ± 0.0007	v_2	0.157 ±0.002	v_3	0.368 ±0.004
T_1	6.68 ± 0.01	T_2	18.75 ±0.01	T_3	3.00 ±0.02

emitted forward with highest energies. The mismatch observed indicates that besides the emission by equilibrated sources, dynamical effects are also present in this region of phase space.

The values of the normalization constants N_1, N_2 and N_3 correspond to the contribution of different sources in the analyzed spectra. To obtain the fractions of neutrons coming from different sources, each of the three functions in eq. (1) was integrated over energies and summed over the detector angles. The results are listed in table 2. Note that these values correspond to the number of registered neutrons and depend on the detector configuration. The contribution of the QT is the largest since, in our case, the target is much heavier than the projectile. All these values are in good agreement with the predictions of the SIMON evaporative model [13] applied to the same reaction and filtered through the same detection system. The small contribution of neutrons from the QP is related to our experimental conditions. Indeed, the smallest measured angle is 8° and the simulation shows that the majority of neutrons coming from the QP is emitted at smaller laboratory angles.

4 Shape of the correlation function

The variation of the source radius and the change of the emission time differently influence the shape of the correlation function. Figure 3a shows two examples of correlation functions for different combinations of the source radius r_0 and the lifetime τ chosen in such a way that they yield

Table 2. Relative contribution in registered neutrons from each emitting source obtained by integration of the fit functions of eq. (1) (middle column) and calculated according to the SIMON model (right column).

	Fit	SIMON model
quasi-target	56 %	57 %
pre-equilibrium	42 %	40 %
quasi-projectile	2 %	3 %

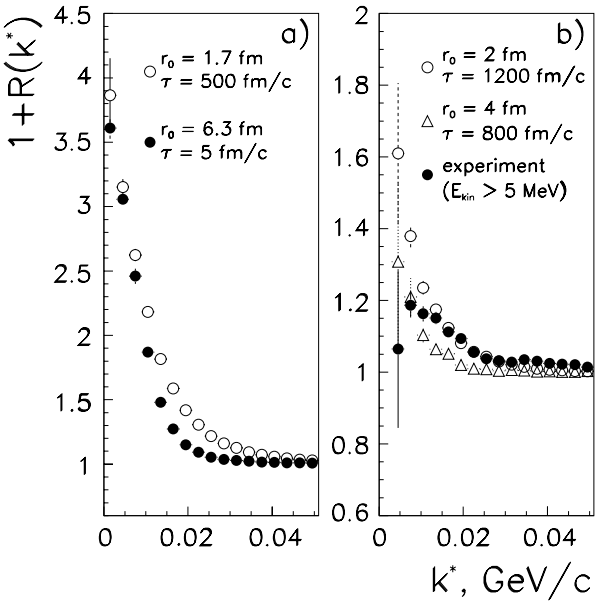

Fig. 3. a) Two correlation functions for different combinations of the source radius r_0 and the lifetime τ; b) comparison of the experimental two-neutron correlation function (for neutrons with $E_{\rm kin}$ >5 MeV; full symbols) with two theoretical correlation functions (open symbols) evaluated for a single source.

the same intercept $R(0)$. The calculations were performed using the code of [14] for a Maxwellian source with a temperature of 5 MeV. Different shapes of correlation functions reflect the interplay between quantum-statistical and final-state-interaction effects for different combinations of space and time parameters. The fact that the form of the correlation function depends on the combination of τ and r_0 gives information about both the source radius and the source lifetime.

Figure 3b illustrates the difficulties arising when comparing the experimental correlation function with the prediction of a single-source Gaussian model. The two generated correlation functions coincide in some points with the experimental one but neither of them agrees with the data all over the exploited k^* region. The single-source approach is clearly insufficient to describe the data.

5 Equilibrated multisource model

Let us assume that neutrons are generated from three sources related to different stages of the collision. The first stage is a rapid emission of high-energy particles (PE source). In the second stage particles are emitted from two low-temperature sources with long lifetimes (QT and QP). The temperatures, velocities and intensities of the sources are chosen from the analysis of inclusive single-neutron spectra. In our case, the number of registered neutrons emitted from the QP is practically negligible (see sect. 3), and, therefore, the generated correlation function is not sensitive to the values of QP parameters.

Thus, only two sources were taken into consideration: a PE and a QT with relative contributions of 57 % and 43 %, respectively. The kinetic energies of the generated particles were sampled from a Maxwellian distribution with the corresponding temperatures. In the source rest frames, the isotropic emission was assumed. The space coordinates of the emission point (x, y, z) were sampled from a spherical Gaussian probability distribution with a dispersion r_0^2. The emission time (t) was taken from an exponential probability distribution $P(t) \sim e^{-t/\tau}$. The values r_0 and τ characterize the space-time dimension of each source. (Note that, in our parameterization, the RMS radius of the source is $\sqrt{3}$ times larger than r_0.) In order to compare the results with the experimental correlation functions, the generated neutrons were filtered through the detection system.

The values of radii and lifetimes were chosen to obtain good agreement with experimental correlation functions simultaneously for three classes of neutrons: with kinetic energies higher than 5 MeV, 10 MeV and 20 MeV. The parameters of the best fit are listed in table 3. The χ^2 values for different τ and r_0 parameters are plotted in fig. 4 for two considered sources. Good agreement between calculations and data is obtained for the PE parameter values of $r_0 = 2.0$–2.2 fm and $\tau = 40$–55 fm/c and for the QT parameter values of $r_0 = 2.6$–3.2 fm and $\tau = 1800$–2600 fm/c.

Table 3. Radii and lifetimes of sources.

	Quasi-target	Pre-equilibrium
r_0	3 fm	2.1 fm
τ	2 000 fm/c	50 fm/c

A comparison of experimental and generated correlation functions is presented in fig. 5. For each energy class, the contribution of registered neutrons coming from different sources is different — the corresponding values obtained from simulations are presented in table 4 and fig. 6. This figure clearly demonstrates that the contributions of the different sources depend not only on the energy cut, but also on the value of the relative momentum of neutron pairs. The strongest k^*-dependence of the different source contribution occurs just in the region of the correlation effect (see fig. 1). Thus, the shape of the correlation function depends in a complicated way on the origin of the two detected neutrons. This stresses that the attempt to describe the shape of the correlation function with a single source of any of the parameters can hardly lead to a positive result.

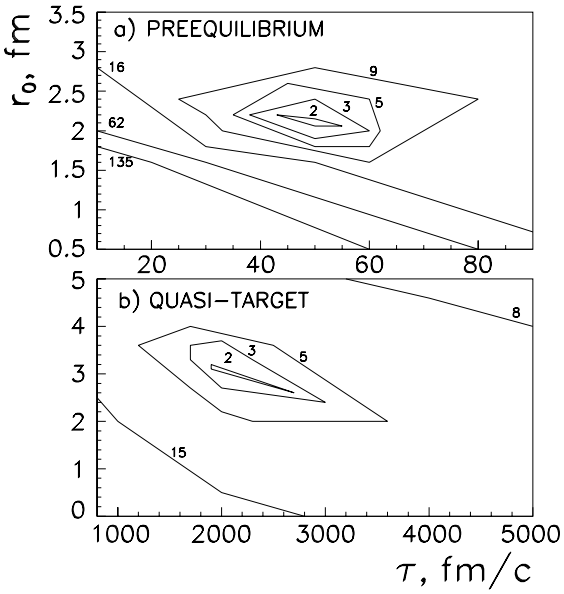

Fig. 4. Contour diagram of χ^2 per degree of freedom determined by comparing the theoretical functions to the data shown in fig. 1 as a function of the pre-equilibrium and the target space-time parameters.

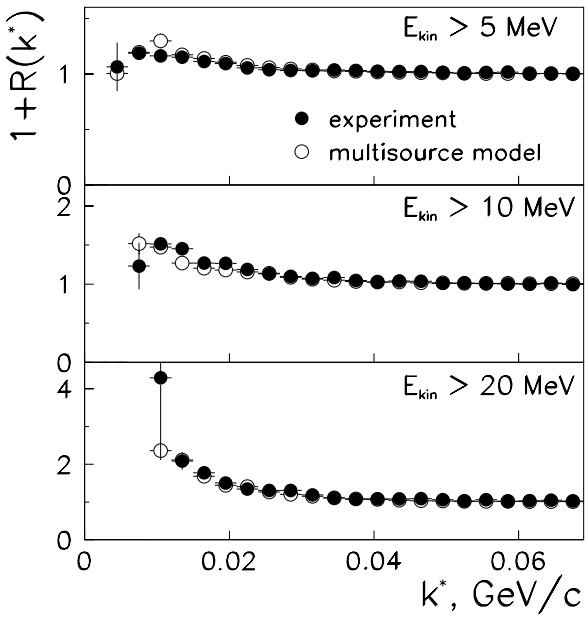

Fig. 5. Experimental two-neutron correlation functions for neutrons with a kinetic energy higher than 5, 10 and 20 MeV, compared with the correlation functions predicted by the equilibrated multisource model. The lifetimes and radii of the sources are presented in table 3.

Table 4. The contribution of registered neutrons from different sources in the three neutron classes (neutrons with a kinetic energy higher than 5, 10 and 20 MeV, respectively).

	$E_{\rm kin}$ >5 [MeV]	$E_{\rm kin}$ >10 [MeV]	$E_{\rm kin}$ >20 [MeV]
pre-equilibrium	43 %	50 %	75 %
quasi-target	57 %	50 %	25 %

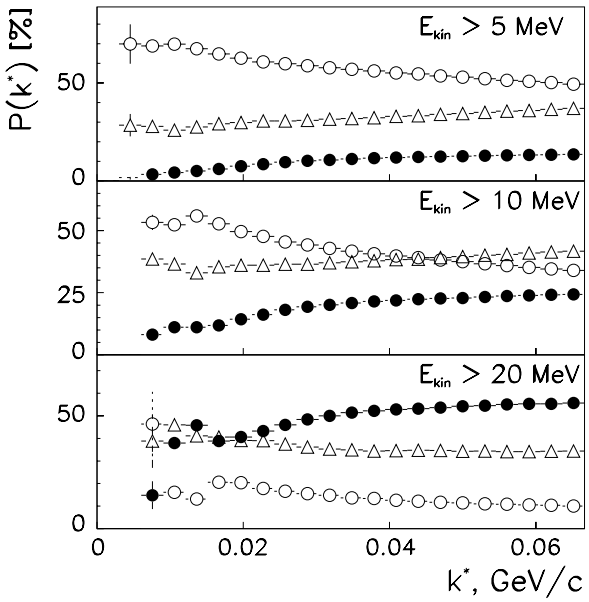

Fig. 6. The k^*-dependence of the relative contribution $P(k^*)$ of neutron pairs coming from different sources: ○ – both neutrons from the QT, ● – both neutrons from the PE, △ – one neutron from the QT another from the PE. Top, middle and bottom panels are for neutrons with a kinetic energy higher than 5, 10 and 20 MeV, respectively.

6 Dynamical model

The correlation functions obtained in the framework of the semiclassical Landau-Vlasov (L-V) approach [15,16] for ^{40}Ar + ^{197}Au at 60 MeV/nucleon are presented in fig. 7. Although the agreement of the model and experimental functions is quite good for neutrons with a kinetic energy higher than 10 and 20 MeV, for neutrons with a kinetic energy higher than 5 MeV the model predicts a stronger correlation effect than obtained in the experiment. The L-V model calculations were carried out up to 800 fm/c. A dynamical calculation can describe an exhaustively long evaporation process very crudely. This results in too small a number of evaporated neutrons and, accordingly, in a shorter average emission time τ. Since the primary QP and QT cool down during the emission process it is, however, likely that the most energetic part of the evaporation spectra is acceptably well predicted by the model. Only 26 % of neutrons come from the QT (∼57 % neutrons come from the first rapid stage of the collision and 17 % from the QP). The deficiency of evaporated neutrons results in disagreement of the theoretical and experimental correlation functions for low-energy neutrons. It must be stressed, however, that this discrepancy can merely be a consequence of the inability of a dynamical model to calculate such a long time. The agreement between the model and the experimental correlation functions for higher-energy neutrons ($E_{\rm kin}$ >20 MeV) coming mainly from the PE indicates that space-time dimensions of this source predicted by the L-V model are reasonably correct. The good agreement for neutrons with the $E_{\rm kin}$ >10 MeV and the disagreement for neutrons with the $E_{\rm kin}$ >5 MeV corroborate our speculation that the higher-energy neutrons are emitted from the QT earlier than the slow neutrons. Thus, the absence of the slowest neutrons in the model which are presumably emitted later than 800 fm/c results in the disagreement of the model and experimental correlation function for $E_{\rm kin}$ >5 MeV.

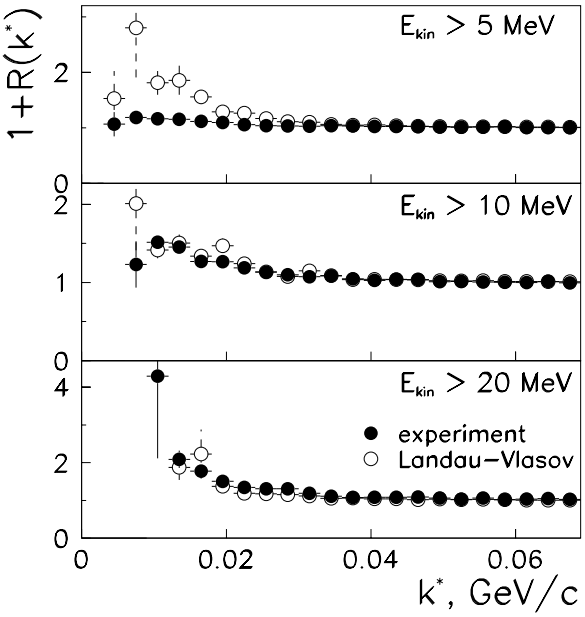

Fig. 7. Experimental two-neutron correlation functions for neutrons with a kinetic energy higher than 5, 10 and 20 MeV, compared with the correlation functions predicted by the semi-classical Landau-Vlasov transport model.

7 Conclusions

It is evidenced that the two-neutron correlation function for the Ar + Au collisions at 60 MeV/nucleon depends strongly on the kinetic energy of the two neutrons. This dependence appears to be basically due to different contributions from different sources. In the frame of the multisource approach considered, registered neutrons come mainly from the pre-equilibrium phase and from the quasi-target disintegration. The temperatures, velocities and the space-time dimensions of the emitting sources have been evaluated.

A comparison of the experimental correlation functions with the prediction of the Landau-Vlasov transport

model indicates good agreement for higher-energy neutrons. Since the model does not incorporate the slow evaporative stage of the reaction, the experimental data concerning the low-energy neutrons cannot be reproduced.

This work was supported by Physics Faculty, Warsaw University of Technology, Grant No. 503 1050 0042 009 and by the GA Czech Republic, Grant No. 202/98/1283.

References

1. B. Erazmus et al., in *Proceedings of the XXXIII International Winter Meeting on Nuclear Physics, Bormio, Italy*, 1996, edited by I. Iori (University of Milan Press, Milan, 1996), p. 149.
2. J. Pluta et al., Nucl. Instrum. Meth. Phys. Res. A **411**, 417 (1998).
3. R. Ghetti, N. Colonna, J. Helgesson, Nucl. Instrum. Meth. Phys. Res. A **421**, 542 (1999).
4. J. Pochodzalla et al., Phys. Rev. C **35**, 1695 (1987).
5. W.G. Gong et al., Phys. Rev. C **43**, 1804 (1991).
6. M. Cronqvist et al., Phys. Lett. B **317**, 505 (1993).
7. N. Colonna et al., Phys. Rev. Lett. **75**, 4190 (1995).
8. S.J. Gaff et al., Phys. Rev. C **58**, 2161 (1998).
9. R. Ghetti et al., LUIP - 9902, Lund (1999).
10. C. Grégoire, B. Remaud, F. Sébille, L. Vinet, Y. Raffray, Nucl. Phys. A **465**, 317 (1987).
11. F.R. Lecolley et al., Nucl. Phys. A **620**, 327 (1997).
12. M. Moszyński et al., Nucl. Instrum. Meth. Phys. Res. A **343**, 563 (1994).
13. D. Durand, Nucl. Phys. A **541**, 266 (1992).
14. R. Lednicky, V. L. Lyuboshitz, Sov. J. Nucl. Phys. **35**, 770 (1982); in *Proceedings of the International Workshop on Particle Correlations and Interferometry in Nuclear Collisions, CORINNE 90, Nantes, France*, 1990, edited by D. Ardouin, (World Scientific, Singapore), 1990, p. 42.
15. Z. Basrak, Ph. Eudes, P. Abgrall, F. Haddad, F. Sébille, Nucl. Phys. A **624**, 472 (1997).
16. Z. Basrak, Nukleonika **43**, 337 (1998).